THE ASTROPHYSICAL JOURNAL, 219:168–182, 1978 January 1

A PHOTOMETRIC STUDY OF THE RECURRENT NOVA WZ SAGITTAE AT MINIMUM LIGHT

EDWARD L. ROBINSON, R. EDWARD NATHER, AND JOSEPH PATTERSON
McDonald Observatory and Department of Astronomy, University of Texas at Austin
Received 1977 February 18; accepted 1977 May 26

ABSTRACT

We have acquired a new set of high-speed photometric observations of the recurrent nova WZ Sge; using these observations, we develop a quantitative model for the system. WZ Sge is a binary system with an orbital period of 81^m38^s and a separation of 3.2×10^{10} cm consisting of an unevolved star with a mass of 0.019 $M_\odot$ orbiting a white dwarf with a mass of 0.38 $M_\odot$. Mass is being transferred from the late-type star to the white dwarf in a stream through the inner Lagrangian point at a rate of 1×10^{16} g s^{-1}. The transferred material forms an accretion disk with a radius of 9.7×10^9 cm around the white dwarf. The accretion disk is optically thick and is the sole source of the broad hydrogen absorption lines seen in the spectrum of WZ Sge. At the point where the stream of transferred material impacts the disk, a bright shock front ("bright spot") is formed. The spot has a radius of 1.0×10^9 cm and an effective temperature near 1.6×10^4 K, and contributes about 15% of the total optical luminosity of the system. In addition, we detect very stable rapid coherent oscillations in the light curve of WZ Sge with periods of 28.98 s and 27.87 s, making WZ Sge the first recurrent nova in which such oscillations have been found. On one occasion both oscillations were present simultaneously in the light curve, and we use this fact to conclude that the rapid oscillations must be pulsations, that the pulsations cannot be radial pulsations, and that the pulsations are probably nonradial *g*-mode pulsations.

Subject headings: stars: binaries — stars: individual — stars: novae

I. INTRODUCTION

WZ Sge is a recurrent nova which erupted in 1913 and 1946, in each case rising about 8 mag from its normal minimum magnitude of 15.5 (Mayall 1946). A considerable body of observational material exists on WZ Sge (e.g., Greenstein 1957; Krzemiński and Kraft 1964; Krzemiński and Smak 1971; Warner and Nather 1972), and confirms that WZ Sge conforms to the canonical model for cataclysmic variables (Robinson 1976*a*): WZ Sge is an eclipsing binary system consisting of a late-type star transferring material to its companion white dwarf. The material is transferred in a discrete stream through the inner Lagrangian point to an accretion disk around the white dwarf. At the point where the stream impacts the accretion disk, a bright shock front ("bright spot") is formed which contributes a significant fraction of the optical luminosity of the system. Several features of the WZ Sge system are unusual: the orbital period is 81^m38^s, with the eclipse lasting only 4 minutes; the ratio of the mass of the white dwarf to the late-type star is large, $q = M_D/M_R \approx 20$; the mass-transfer rate is low, $\dot{M} \approx 10^{16}$ g s^{-1}; and, as opposed to other cataclysmic variables, the bright spot is visible even when on the opposite side of the disk from the observer.

An improved knowledge of the WZ Sge system is of considerable importance. WZ Sge is a cornerstone in our knowledge of the structure of cataclysmic variables. WZ Sge is near the end of its lifetime as a cataclysmic variable, and provides insight into one of the possible end states of the evolution of these systems. Kraft, Mathews, and Greenstein (1962), Paczyński (1967), and Faulkner (1971) have suggested that the evolution of WZ Sge is dominated by angular momentum loss due to gravitational radiation, and that WZ Sge may eventually provide a test of the theory of gravitational radiation. We have therefore acquired a new set of high-speed photometric observations of WZ Sge; using these observations, we develop a quantitative model for WZ Sge, and, in particular, we provide unambiguous masses and dimensions for the system. In addition, we find coherent oscillations in the light curve with periods of 27.87 and 28.98 s. We show that the properties of the oscillations are inconsistent with any mechanism which invokes rotation of the white dwarf as their source. Instead, the oscillations appear to be caused by nonradial *g*-mode pulsations of the white dwarf.

II. THE OBSERVATIONAL DATA

The light curves of WZ Sge were acquired during 1971 and 1976 with the 82 inch (2.1 m) telescope at McDonald Observatory, using the McDonald high-speed photometer (Nather 1973). The data were gathered by using our standard observational techniques (Nather and Warner 1971), except that unusual care was taken to avoid contamination of the light curve of WZ Sge by light from the bright star 7″ away. We used field apertures with diameters of either 7″ or 10″, and observed WZ Sge only on nights with very

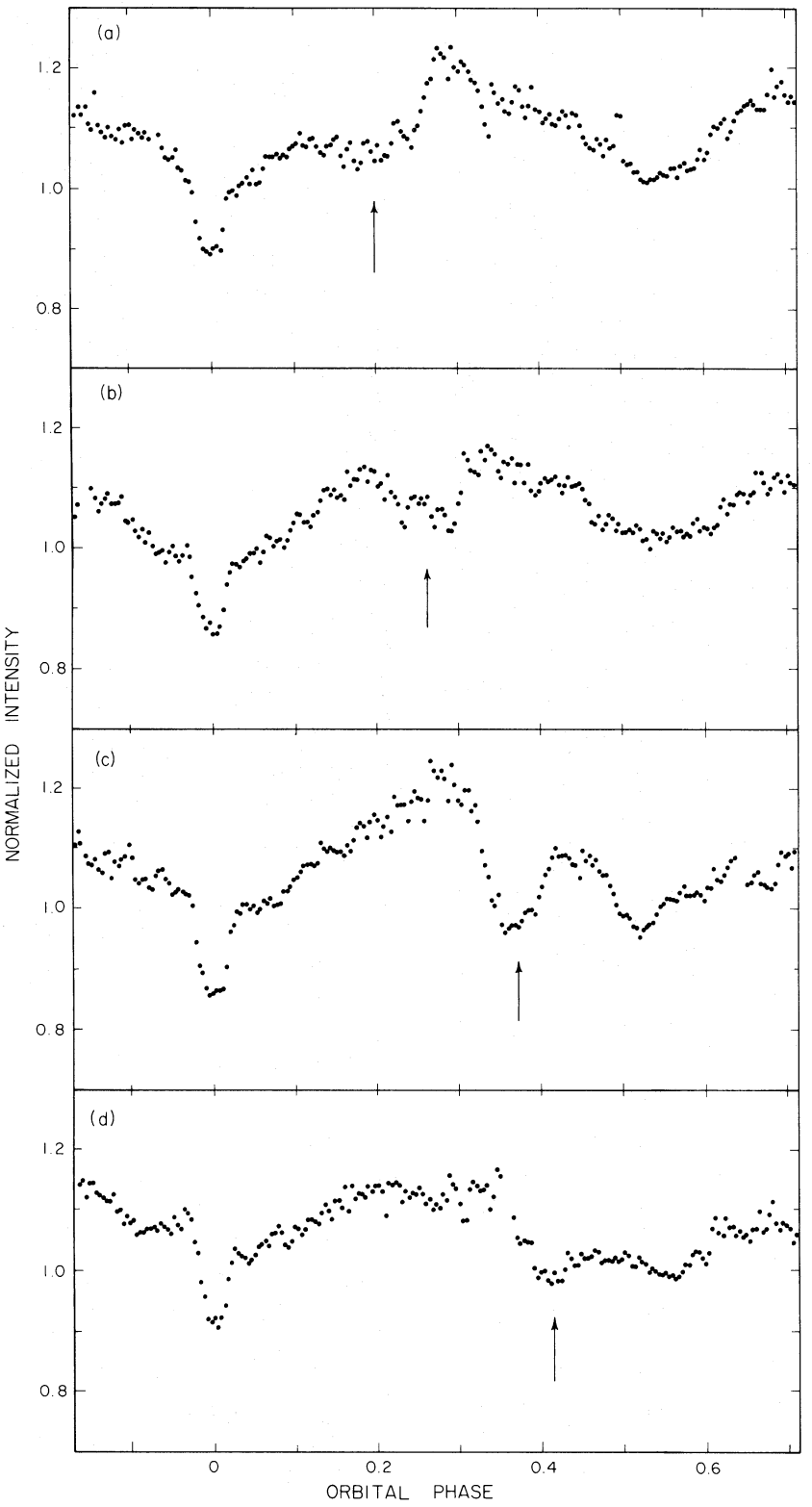

FIG. 1.—The light curve of WZ Sge for eclipse numbers (see Table 2): (*a*) 96387, (*b*) 94978, (*c*) 97021, (*d*) 94960. Each light curve has been separately normalized so that an intensity of 1.0 corresponds approximately to the light level at the minima of the W Ursae Majoris part of the light curve. Each point is the mean intensity averaged over 20 s. The arrows mark the approximate midpoint of the "dips" which are superposed on the W Ursae Majoris maximum immediately following the primary eclipse.

TABLE 1

JOURNAL OF OBSERVATIONS

Run Number	Run Start $JD_\odot$ 2440000+	Integration Time (s)	Number of Integrations
1203.....	1208.62856	1	10420
1208.....	1210.59824	3	2150
1736.....	2930.78910	5	2750
1739.....	2931.79176	5	2610
1760.....	3011.63826	5	3190
1768.....	3013.67859	5	2500
1770.....	3041:65873	5	1070
1773.....	3047.60306	5	2170

good seeing. The observations were made in white light with a variety of blue-sensitive bi-alkali photomultiplier tubes, and with integration times ranging from 1 to 5 s. Details of the individual runs are given in Table 1. A preliminary presentation of the two runs acquired in 1971 has already been given (Warner and Nather 1972), and we refer the reader to the figures presented in that paper for additional examples of time-resolved light curves of WZ Sge.

In Figure 1, the portion of the light curve of WZ Sge running from orbital phases 0.85 to 0.70 is shown for four different orbital cycles. The major features of the light curve are: a narrow and variable primary eclipse from which phase zero is defined; the double-humped W Ursae Majoris–type variation, of which only the hump peaking near phase 0.30 is completely shown in Figure 1; and the deep and highly variable "dips" in the W Ursae Majoris hump, which are pointed out by the arrows in Figure 1.

Eclipse number 94961 (see Table 2 for the Julian dates of the eclipse numbers), shown in expanded form in Figure 2, is a typical example of the primary eclipse. The eclipse is very narrow. The mean time between first and fourth contacts, Δt_{14}, is 238 s, but the width can vary from 195 s to 275 s in the most extreme cases we have observed. The eclipse depth is

TABLE 2

PRIMARY ECLIPSE DATA

Eclipse Number	Mid-Eclipse $JD_\odot$ 2440000+	Δt_{14} (s)	Δt_{23} (s)	$\Delta t_{1/2}$ (s)
64581.....	1208.68628	195	70	145
64582.....	1208.74296	220	85	160
64615.....	1210.61352	258	78	174
94960.....	2930.80629	245	55	165
94961.....	2930.86297	230	65	165
94962.....	2930.91962	Partial Eclipse		
94978.....	2931.82664	250	55	167.5
94979.....	2931.88325	232.5	55	165
94980.....	2931.94002	232.5	55	145
96387.....	3011.69971	230	100	165
96388.....	3011.75643	Partial Eclipse		
96389.....	3011.81320	245	80	170
96422.....	3013.68393	225	80	162.5
96423.....	3013.74059	270	75	162.5
96424.....	3013.79724	215	80	152.5
97021.....	3047.63991	275	80	187.5
97022.....	3047.69645	240	85	172.5

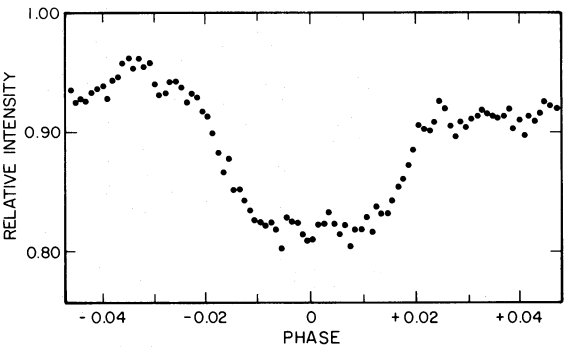

FIG. 2.—The primary eclipse number 94961 of WZ Sge. The intensity level is given in arbitrary relative intensity units. Each point is the mean intensity averaged over 5 s.

also variable, ranging from about 0.10 to 0.16 mag deep in our data. The multicolor photometry of WZ Sge obtained by Krzemiński and Smak (1969, 1971) shows that the eclipse depth is strongly color-dependent, with mean depths of $\Delta U = 0.24$ mag, $\Delta B = 0.16$ mag, and $\Delta V = 0.18$ mag. The primary eclipse is always asymmetric, with ingress typically lasting about 100 s, and egress lasting about 70 s. The magnitude change during ingress is about 25% larger than that of egress. The extent of the asymmetry varies considerably from eclipse to eclipse, and in some cases becomes small enough to be barely detectable; for an example of a nearly symmetric eclipse, see the lower curve of Figure 4 in Warner and Nather (1972). All but two of the 17 primary eclipses we measured were flat-bottomed, and thus were total eclipses. The time between second and third contacts is quite short, typically 50 s to 100 s. Krzemiński and Smak (1971) were unable to recognize that the eclipse is total because of the lower time resolution of their photometry, and they assumed that the eclipse was a partial eclipse. Many of the differences in the model parameters we derive for WZ Sge from those derived by Krzemiński and Smak stem from this difference in the adopted nature of the eclipse.

The W Ursae Majoris part of the light curve consists of two nearly but not exactly equal humps, each one lasting about half the orbital period. The hump just prior to primary eclipse has a slightly sharper and earlier decline to minimum than the hump after primary minimum. In our data the amplitude of the humps is about 0.18 mag, but once again, the multicolor photometry of Krzemiński and Smak (1971) shows that the amplitude has a strong wavelength dependence, with mean amplitudes of $\Delta U = 0.18$ mag, $\Delta B = 0.12$ mag, and $\Delta V = 0.08$ mag. The W Ursae Majoris variation is displaced somewhat from the primary eclipse, but the exact amount of the displacement depends on how the displacement is measured. The most easily defined part of the W Ursae Majoris variation, the minimum which is at phase 0.5, gives a displacement of about 0.046 in phase in both our observations and those of Krzemiński and Smak. There is considerable flickering activity in the light curve near the peak of the W Ursae Majoris humps.

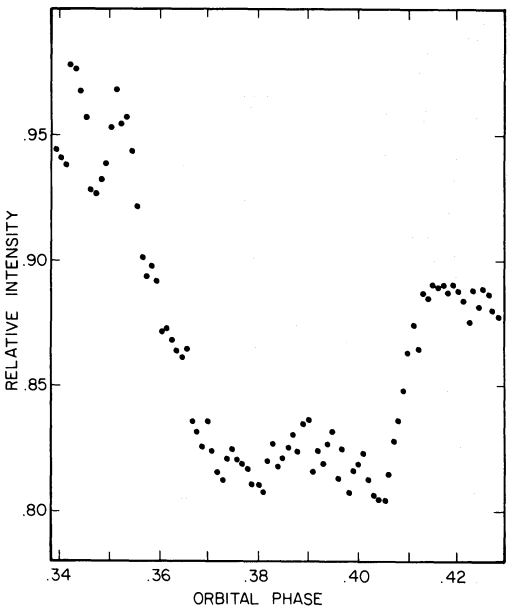

FIG. 3.—The extremely rapid dip which was observed following primary eclipse number 94961. The intensity level is given in arbitrary relative intensity units. Each point is the mean intensity averaged over 5 s.

The flickering at these phases has an amplitude of up to 0.10 mag, and a time scale for decay of about 30 s. The flickering is evident only as an increased noise in the light curves shown in Figure 1 because the flickering is not time-resolved by the 20 s data points. Figure 3 of Warner and Nather (1972) gives the appearance of the flickering when it is adequately time-resolved. According to Warner and Nather (1972), the flickering has a larger amplitude on the hump prior to primary eclipse, but from our larger data base it would appear that this asymmetry, if present, is very small. The flickering has a much lower amplitude during the minima of the W Ursae Majoris variation.

The dips are superposed on the W Ursae Majoris hump immediately following primary eclipse, and never occur on the hump prior to the eclipse. We have seen a dip on each of the 15 orbital cycles which we observed at the proper orbital phase, which indicates that the dips occur in a more regular way than previously thought. The details of the dips vary over a wide range. The center of the dips can occur earlier than phase 0.20 and later than phase 0.40, and the width of the dips can vary from $\Delta\phi = 0.06$ to at least $\Delta\phi = 0.10$. Figure 3 displays one of the most extreme dips we have observed. The decrease in light takes only 90 s; there follows a period of nearly constant luminosity lasting about 160 s; and then the rise back to normal light takes only about 40 s. The light level at the center of the dips is, with occasional exceptions, approximately the same as the light level at the minima of the W Ursae Majoris variation. Thus the visual effect of the dips on the light curve is that part of the W Ursae Majoris hump has been "chopped out" of the light curve.

The spectrum of WZ Sge shows a strong blue continuum with weak hydrogen emission lines (Humason 1938). The hydrogen emission lines are very broad, doubled, and superposed on yet broader, but very weak, absorption lines which are reminiscent of those of a DA white dwarf (McLaughlin 1953; Greenstein 1957). The double peaks are separated by about 1440 km s^{-1}, and have no detectable orbital radial-velocity variations; the upper limit on the semi-amplitude of the variations is $K \leqslant 40$ km s^{-1} (Krzemiński and Kraft 1964). An unusual feature of the emission line is a third, "S-wave" component with a variable radial velocity (Kraft 1961, 1964; Krzemiński and Kraft 1964). The radial velocity of the S-wave component varies periodically, but not exactly sinusoidally, at the orbital period. The amplitude of the radial-velocity variation ranges from 650 km s^{-1} to 850 km s^{-1}, but on average is similar to one-half the separation of the stationary double components. The phase of the radial velocity of the S-wave component is such that it reaches maximum recessional velocity about 0.06 in phase after primary eclipse. On single trailed photographic spectrograms, this third emission component has the appearance of an S—whence its name: S-wave.

III. THE ORBITAL PERIOD

Since the total time base covered by the observations is now nearly twice that available to Krzemiński and Smak (1971), we are able to improve significantly their eclipse ephemeris. The data consist of the eclipse timings published by Krzemiński and Kraft (1964), Krzemiński and Smak (1971), and Mumford (1969, 1971, and 1974), plus the new timings from our data. Since the eclipses are asymmetric, there is no well-defined time of mid-eclipse, and various definitions of mid-eclipse can give systematic differences in timings of up to about 10 s. We define mid-eclipse in our data as follows: find the times during the eclipse ingress and egress when the light level has changed by one-half the total change; mid-eclipse is the average of these two times. The resultant eclipse timings are listed in column (2) of Table 2. As noted previously by Krzemiński and Smak (1971), Mumford's eclipse timings give systematically positive residuals in the O-C diagram. Therefore we have excluded his data from the ephemeris calculation. The best linear fit to the eclipse timings is

$$T = \mathrm{JD}_{\odot}\ 2437547.72845 \pm 3 + 0^{d}.0566878455 \pm 7\,E, \quad (1)$$

where T is the heliocentric Julian date of mid-eclipse, and E is the eclipse number. There is no evidence for any period change; the 3 σ upper limit on the rate of change of the period is $|\dot{P}| < 4 \times 10^{-12}$. The resulting O-C diagram for the eclipse timings is shown in Figure 4. It should be noted that the primary eclipse is very stable in phase. From eclipse number 31000 on, the largest single residual, except for Mumford's timings, is 21 s. The standard deviation of an individual timing is only 8 s. Measurement errors rather than a true

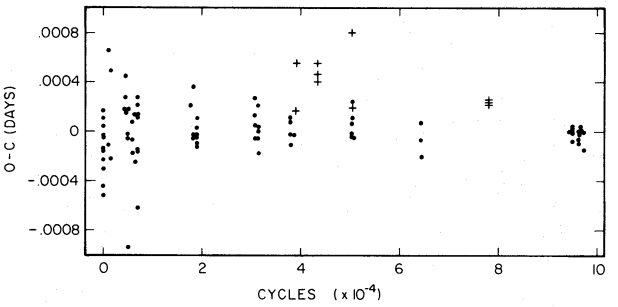

FIG. 4.—The O-C diagram for the eclipse timings of WZ Sge calculated using the ephemeris given by eq. (1). Mumford's eclipse timings are denoted by crosses. They have a systematically positive residual and have been excluded from the calculation of the ephemeris.

variation in eclipse timings must be considered the major source of residuals this small.

IV. THE MODEL OF WZ SAGITTAE

a) Qualitative Description of the Model

The geometry of the basic model for WZ Sge, shown in Figure 5, is qualitatively similar to the model proposed by Krzemiński and Smak (1971). The detailed arguments which lead to this model have been presented more than adequately by Krzemiński and Kraft (1964), Krzemiński and Smak (1971), and Warner and Nather (1972), and we will not repeat them here. In brief, the late-type star is invisible, and, as we shall see, the white dwarf is only a minor contributor to the total luminosity of the system. The optical luminosity of the system is almost totally dominated by the accretion disk and the bright spot. The primary eclipse is an eclipse of the bright spot by the late-type star, and the variations in the shape and the depth of the eclipse are caused by variations in the size and position of the spot. Since the spot is a shock front caused by the impact of the stream of transferred material with the disk, it lies along the stream trajectory, which is nearly parallel to the line joining the spot to the center of the late-type star. Thus, one of the few stable features of the eclipse is the time of mid-eclipse. The luminosity of the spot varies irregularly, perhaps because of inhomogeneities in the stream or the disk, and gives rise to the rapid flickering. The scale height of the disk is significantly larger at the radius of the spot than it is just interior to the spot, so that the disk looks somewhat like a thick ring connected to the white dwarf by a thin hub. The spot also has a large scale height. It is this geometry which gives rise to the W Ursae Majoris variation in the light curve. Since the spot extends above the inner regions of the disk, it can be seen both when on the side of the disk facing the observer and when on the side opposite the observer, thus producing the maxima of the W Ursae Majoris variation. When viewed at 90° to these two phases, light from the spot must pass through the extra disk material in the extended ring. The spot is then partially obscured, which produces the minima of the W Ursae Majoris variation. The spot cannot be totally obscured because the primary eclipse occurs during one of the minima of the W Ursae Majoris variation. A comparison of the height of the humps of the W Ursae Majoris variation with the depth of the primary eclipse suggests that the apparent brightness of the spot is reduced by about 40% at the W Ursae Majoris minima. Since the spot is the source of the flickering, the amplitude of the

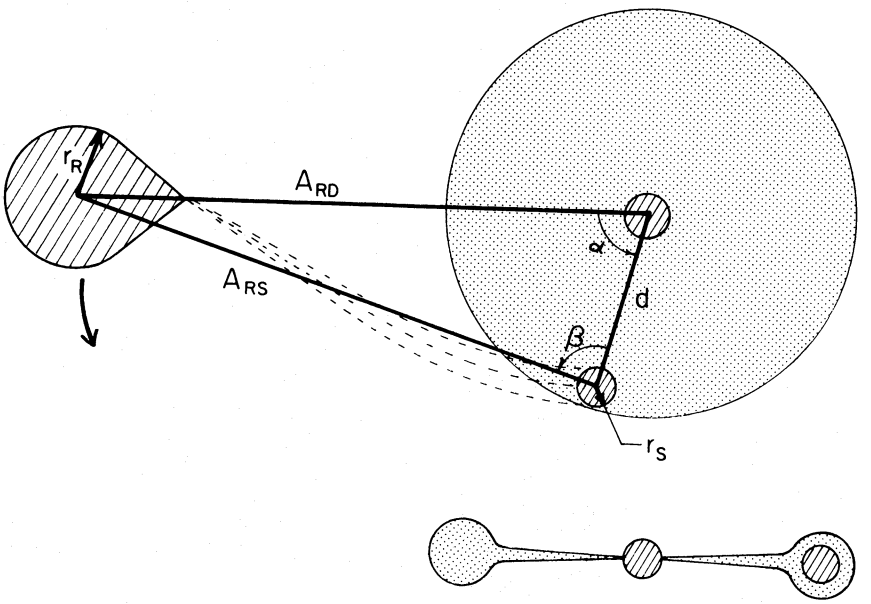

FIG. 5.—*Upper figure*, geometry of the WZ Sge system as seen from above the orbital plane. *Lower figure*, geometry of the disk as seen from the plane of the disk.

flickering also decreases at the minima, and disappears almost entirely during primary eclipse. In principle, the spot could be somewhat elongated along the circumference of the disk, and if so, perspective would foreshorten the spot and further decrease its apparent brightness at the minima of the W Ursae Majoris variation. This effect is of only minor importance in WZ Sge, since we shall find that the adoption of a circular cross section for the spot gives internally consistent results. The asymmetry of the primary eclipse is chiefly due to the same geometry which produces the W Ursae Majoris variation, but once again, if the spot is elongated, foreshortening could contribute to the asymmetry. The displacement of the W Ursae Majoris variation from primary eclipse by $\Delta\phi = 0.046$ is a measure of β, the angle from the spot to the white dwarf. The disk proper, as opposed to the spot, is also partly eclipsed, but the disk eclipse is very shallow, broad, and difficult to detect because it is superposed on the large amplitude of W Ursae Majoris variation. The only feature in the light curve which is clearly attributable to the disk eclipse is the premature decline of the W Ursae Majoris hump prior to primary eclipse.

The stationary double-peaked emission lines are produced by the disk of gas, and as shown by Smak (1969) and Huang (1972), one-half the separation of the peaks corresponds closely to the projected radial velocity of the outer edge of the disk. Smak (1976) has recently proposed that the S-wave component in the spectrum of the dwarf nova U Gem comes from the stream of transferred material, and he suggests that this is also the case in WZ Sge. However, we believe that the original model proposed by Krzemiński and Smak (1971), in which the S-wave component comes from the spot or regions of the disk very near the spot, in fact is correct, because the phase of the S-wave component matches the phase of the W Ursae Majoris variation very closely. The amplitude of the S-wave radial-velocity curve is equal, on average, to the separation of the stationary double-peaked emission, so the spot is, on average, at the outer edge of the disk. It has generally been assumed that the broad absorption wings on the hydrogen line profiles are the wings of normal hydrogen absorption lines from the white dwarf. We shall show that this assumption is not justified, and that the lines are produced by the accretion disk.

b) Analysis of the Primary Eclipse

Because the primary eclipse is total, we can derive from it the orbital inclination, i, the relative radius of the late-type star, r_R/A_{RS}, and the relative radius of the

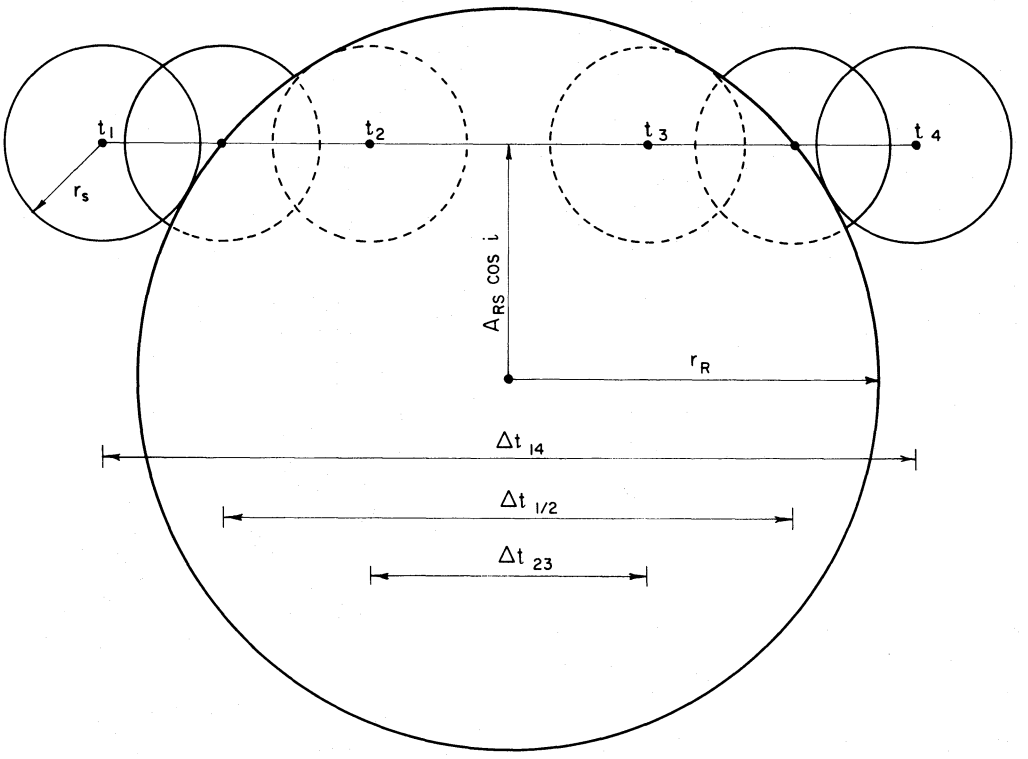

FIG. 6.—The adopted geometry for the primary eclipse. The eclipse is a total eclipse; t_1, t_2, t_3, and t_4 are the times of first, second, third, and fourth contacts. The late-type star and the spot both have circular cross sections with radii which remain constant over the course of the eclipse. The radii are very much less than their separation, A_{RS}. The orbital inclination, i, and Δt_{14} and Δt_{23} have their usual definitions. The quantity $\Delta t_{1/2}$ is the interval between the times on ingress and egress when the center of the spot passes the limb of the late-type star. The relative dimensions shown in this figure are similar to the dimensions we actually derive.

bright spot, r_S/A_{RS}, where A_{RS} is the separation of the spot and the late-type star (see Fig. 5). Our model for the primary eclipse is rather crude, but a greater sophistication is not warranted, since the data, not the model, will set the limit to the accuracy of our results. The geometry for the primary eclipse is shown in Figure 6. The eclipse is a total eclipse, with t_1, t_2, t_3, and t_4 being the times of first, second, third, and fourth contacts. The late-type star and the spot both have circular cross sections with radii which remain constant for the duration of the eclipse. The radii are very much less than their separation, and the radius of the spot is much less than the radius of the late-type star. The quantity $\Delta t_{1/2}$ is the interval between the times on ingress and egress when the center of the spot passes the limb of the late-type star. Since the radius of the spot is assumed to be much less than the radius of the late-type star, $\Delta t_{1/2}$ can be measured from the points on ingress and egress when the light level has changed by one-half the total change. In addition, we assume that the orbit is circular, and that the spot has a uniform surface brightness. It might be objected at this point that, although the model we have adopted can give only symmetric eclipses, the observed eclipses are always at least slightly asymmetric. In order to test the significance of this problem, we divided the eclipses into two groups, one group consisting of nearly symmetric eclipses, the other consisting of very asymmetric eclipses. The results obtained from the two groups differed by much less than the formal errors. Thus we do not believe that the asymmetry of the eclipse introduces any significant errors into our results. It might also be objected that our approximate technique for measuring $\Delta t_{1/2}$ introduces an unacceptably large systematic error in $\Delta t_{1/2}$ and therefore in the orbital inclination. We calculate that, for our model of WZ Sge, the approximation will make the inclination systematically too large, but by no more than 3°. This error is sufficiently small, and we make no correction for it.

The following relations can be easily derived from the geometry shown in Figure 6:

$$\Delta t_{14}{}^2 = \frac{P^2}{\pi^2}\left[\left(\frac{r_R}{A_{RS}} + \frac{r_S}{A_{RS}}\right)^2 - \cos^2 i\right]; \quad (2)$$

$$\Delta t_{23}{}^2 = \frac{P^2}{\pi^2}\left[\left(\frac{r_S}{A_{RS}} - \frac{r_S}{A_{RS}}\right)^2 - \cos^2 i\right]; \quad (3)$$

$$\Delta t_{1/2}{}^2 = \frac{P^2}{\pi^2}\left[\left(\frac{r_R}{A_{RS}}\right)^2 - \cos^2 i\right]. \quad (4)$$

The orbital period, P, and Δt_{14}, Δt_{23}, and $\Delta t_{1/2}$ are all directly measurable. Thus we have three equations which can be solved for the three unknowns, r_R/A_{RS}, r_S/A_{RS}, and i.

The measured values of Δt_{14}, Δt_{23}, and $\Delta t_{1/2}$ for each eclipse are listed in Table 2. In practice, the results for the individual eclipses are sensitive to errors in the measured values of the time intervals. It is not possible to reduce the errors simply by averaging together all of the time intervals from the individual eclipses, since we expect r_R/A_{RS} and r_S/A_{RS} to vary from eclipse to eclipse. However, the orbital inclination will be constant. Therefore we have solved equations (2)–(4) as follows. Using the tabulated values of the time intervals, we solve equations (2)–(4) simultaneously to get the orbital inclination for each eclipse individually, and then take the average to get the best estimate for the inclination. The result is $i = 84\overset{\circ}{.}6 \pm 1\overset{\circ}{.}0$. Using this inclination and equation (4), we calculate r_R/A_{RS} for each eclipse individually. On doing this, we find that r_R/A_{RS} is also constant; the true variations are less than the scatter due to measurement error. Therefore we take the average of the individual values of r_R/A_{RS} and obtain $r_R/A_{RS} = 0.141 \pm 0.012$. Knowing i and r_R/A_{RS}, we can now calculate r_S/A_{RS} for the individual eclipses from either equation (2) or equation (3). Thus we have absorbed all of the variations in the eclipses into variation of the radius of the spot. The mean radius of the spot is $r_S/A_{RS} = 0.037$, but the radius varies by more than a factor of 2, from 0.025 to greater than 0.050. For radii greater than 0.050, the eclipse becomes partial.

c) *The Relative Geometry and the Mass Ratio*

The angle, β, from the spot to the white dwarf is given by the displacement of the W Ursae Majoris variation from the primary eclipse: $\beta = \pi/2 + \Delta\phi = 106\overset{\circ}{.}5$. We cannot proceed further than this on purely observational grounds; theory must provide us with one, but only one, relation among the remaining properties of the model. Of the various relations which suggest themselves for consideration, we have chosen

$$\frac{d}{A_{RD}} = f(q): \quad (5)$$

that is, the relative distance of the spot from the white dwarf is a function only of the mass ratio. We have chosen this function partly because it is simple, but primarily because it is essentially a statement of conservation of angular momentum, and thus comparatively insensitive to the details of the physics used to derive it. The function does not exist in analytic form; it must be tabulated. Tables for equation (5) have been published by Flannery (1975) and Lubow and Shu (1975). We use the Lubow and Shu results. The geometry of the model gives two additional relations:

$$1 = \left(\frac{d}{A_{RD}}\right)^2 + \left(\frac{A_{RS}}{A_{RD}}\right)^2 - 2\left(\frac{d}{A_{RD}}\right)\left(\frac{A_{RS}}{A_{RD}}\right)\cos\beta, \quad (6)$$

$$\frac{r_R}{A_{RD}} = \left(\frac{r_R}{A_{RS}}\right)\left(\frac{A_{RS}}{A_{RD}}\right). \quad (7)$$

Finally, since the late-type star is transferring matter to the white dwarf, it must both fill its Roche lobe and have the shape of its Roche lobe. The relative dimensions of the Roche lobe are a function only of the mass ratio. Since r_R/A_{RS} was measured from the primary eclipse, the appropriate dimension to use is the radius

of the Roche lobe as measured in the plane of the orbit and at right angles to the line joining the late-type star to the white dwarf. Tables of this radius, and an approximate analytic fit to the table, have been given by Plavec and Kratochvil (1964), but we cannot use their analytic fit because it is inaccurate at the extreme mass ratios appropriate for WZ Sge. Instead, we have made the following fit to their table:

$$q^{-1} = 48.765\left(\frac{r_R}{A_{RD}}\right)^3 - 14.320\left(\frac{r_R}{A_{RD}}\right)^2 + 1.4321\left(\frac{r_R}{A_{RD}}\right). \quad (8)$$

Although somewhat cumbersome to use, equation (8) is accurate to a few percent over the range $0 \leq q^{-1} \leq 1$. Since β and r_R/A_{RS} are known, the four equations (5) to (8) can be solved for the four unknowns, q, d/A_{RD}, r_R/A_{RD}, and A_{RS}/A_{RD}. The solutions to the equation is straightforward, but because the mass ratio turns out to be quite large, we had to extrapolate somewhat beyond the end of the table for equation (5) given by Lubow and Shu. The variation of d/A_{RD} with q is both slow and smooth, so the extrapolation presents no additional problem.

Solution of equations (5) to (8) yields $q = 19.9$, $d/A_{RD} = 0.303$, $A_{RS}/A_{RD} = 0.871$, and $r_R/A_{RD} = 0.123$. Straightforward calculation now gives, in addition, $r_S/A_{RD} = 0.032$, and $\alpha = 56°.5$.

d) *The Masses and the Absolute Dimensions*

The outer edge of the accretion disk is sufficiently close to the white dwarf that its motion should be very nearly circular and Keplerian. As we have already noted, the spot is at the outer edge of the disk. Thus the radius of the disk is also d, and the velocity at its outer edge is $v \sin i = 720$ km s^{-1}, or $v = 725$ km s^{-1}. For the binary orbit, Kepler's law gives

$$GM_D\left(\frac{1+q}{q}\right) = \frac{4\pi^2}{P^2} A_{RD}{}^3. \quad (9)$$

The velocity of the outer edge of the disk is

$$v^2 = \frac{GM_D}{d}. \quad (10)$$

Combining equations (9) and (10), we obtain

$$M_D = v^3\left(\frac{1+q}{q}\right)^{1/2}\left(\frac{d}{A_{RD}}\right)^{3/2}\frac{P}{2\pi G}. \quad (11)$$

All the parameters on the right-hand side of equation (11) are known, and we obtain $M_D = 7.6 \times 10^{32}$ g $= 0.38\ M_\odot$. Inserting this mass into equation (9) then gives $A_{RD} = 3.2 \times 10^{10}$ cm. The rest of the geometry, and the mass of the late-type star, follow immediately: $M_R = 0.019\ M_\odot$, $A_{RS} = 2.8 \times 10^{10}$ cm, $d = 9.7 \times 10^9$ cm, $r_R = 3.9 \times 10^9$ cm, and $r_S = 1.0 \times 10^9$ cm. Using $r_D = 7.0 \times 10^8$ cm $(M_D/M_\odot)^{-1/3}$, we find that the radius of the white dwarf is $r_D = 9.7 \times 10^8$ cm. The properties of WZ Sge are summarized in Table 3.

TABLE 3

SUMMARY OF THE PROPERTIES OF WZ SAGITTAE

Parameter	Units	Value
T_0	JD$_\odot$	2437547.72845 ±3
P	Days	0.0566878455 ±7
$\lvert\dot{P}\rvert$	Unitless	$< 4 \times 10^{-12}$ (3 σ)
i	Degrees	84.6 ± 1.0
M_D	$M_\odot$	0.38
M_R	$M_\odot$	0.019
q	M_D/M_R	19.9
$\dot{M}$	g s^{-1}	1×10^{16}
A_{RD}	cm	3.2×10^{10}
A_{RS}	cm	2.8×10^{10}
d	cm	9.7×10^9
r_R	cm	3.9×10^9
r_s	cm	1.0×10^9
r_D	cm	9.7×10^8
α	Degrees	56.5
β	Degrees	106.5
T_{se}	K	1.6×10^4

We hesitate to assign specific confidence limits to any of the numbers in Table 3, since the chain of logic by which they were derived is rather long. We believe that the absolute geometry and the mass ratio are accurate to about 10%, and that the relative geometry is accurate to better than 10%; but the masses of the stars are very sensitive to inaccuracies in the radial velocity and the relative radius of the disk. They could easily be in error by 30% or more. The two previous major investigations of WZ Sge, those of Krzemiński and Kraft (1964) and Krzemiński and Smak (1971), used different sets of data, adopted different sets of physical assumptions, and used different analysis techniques from those of our investigation. Yet their results are surprisingly similar to ours. In the case of the *least* accurate numbers, the masses of the two stars, Krzemiński and Kraft give $M_D = 0.59\ M_\odot$ and $M_R = 0.03\ M_\odot$, and Krzemiński and Smak give $M_D = 0.35\ M_\odot$ and $M_R = 0.025\ M_\odot$. The only discrepant mass determination is that of Warner (1973), but his explicit assumption that the late-type star fits the lower-main-sequence mass-radius relation is inappropriate, since unevolved stars with masses less than $0.07\ M_\odot$ are not burning hydrogen, and cannot be expected to fit a mass-radius relation for hydrogen-burning stars. This comparison of the mass determinations for WZ Sge suggests that we have converged on a reasonably accurate model for the system. Nevertheless, we caution the reader not to accept our results and error estimates too readily, since they depend heavily on the adopted model for WZ Sge. Small changes in the model may cause large changes in the derived masses of the stars.

e) *The Structure of the Disk*

The fundamental parameter needed to discuss the structure of the disk is the mass-transfer rate. The rate of change of the orbital period gives an upper limit to the transfer rate. Assuming conservation of mass and

orbital angular momentum, and assuming that the orbit of WZ Sge is circular, we have

$$\dot{M} = \frac{-\dot{P}}{P}\frac{M_R M_D}{3(M_D - M_R)} . \quad (12)$$

When we use the upper limit on $\dot{P}$ found in § III, equation (12) yields $\dot{M} < 1.7 \times 10^{-10}\, M_\odot\ \mathrm{yr}^{-1} = 1.1 \times 10^{16}\ \mathrm{g\ s}^{-1}$. A moderate loss of mass and angular momentum from the system may change this upper limit by perhaps a factor of 2.

We may also estimate the mass-transfer rate from the luminosity of the spot. According to Greenstein (1957), the absolute visual magnitude of WZ Sge is about +10.5. As measured from the primary eclipse, the spot contributes about 15% of this luminosity, so the absolute visual magnitude of the spot is about +12.5. We shall calculate later that the temperature of the spot must be in the range of 15,000–20,000 K. We adopt, then, a bolometric correction for the spot of 1.7 mag, and we find the luminosity of the spot to be $L_{\mathrm{spot}} = 1.4 \times 10^{31}\ \mathrm{ergs\ s}^{-1}$. If the available kinetic energy of the stream of transferred material is converted completely to light, the mass-transfer rate is given by

$$\dot{M} = \frac{2dL_{\mathrm{spot}}}{GM_D} . \quad (13)$$

The mass-transfer rate is then $\dot{M} = 5 \times 10^{15}\ \mathrm{g\ s}^{-1}$.

We consider the mass-transfer rate derived from the spot luminosity to be a lower limit, because the spot is embedded in the disk and must radiate more effectively in the direction perpendicular to the disk. Since we observe WZ Sge from the plane of the disk, we have underestimated the total luminosity of the spot. Therefore we adopt $\dot{M} = 1.0 \times 10^{16}\ \mathrm{g\ s}^{-1}$ as the best estimate of the transfer rate.

In spite of the broad hydrogen absorption lines in the spectrum of WZ Sge, the white dwarf must be a minor contributor to the total luminosity of the system for two reasons. First, with our geometry for WZ Sge, the white dwarf is eclipsed, and the eclipse should be $\Delta\phi = -0.046$ before the primary eclipse. Reference to Figures 1 and 2 shows that the eclipse is either shallow or nonexistent, so the white dwarf is faint. Second, based on the available potential energy, the ratio of the luminosity of the disk to the luminosity of the spot should be $L_{\mathrm{disk}}/L_{\mathrm{spot}} \approx d/r_D \approx 10$. The spot contributes about 15% of the total optical luminosity from WZ Sge, and thus the combination of spot plus disk luminosity more than accounts for the total luminosity of the system.

Since the white dwarf is a minor contributor to the total luminosity of WZ Sge, the white dwarf cannot be the source of the broad hydrogen absorption lines. It has occasionally been suggested that the broad hydrogen absorption lines seen in other cataclysmic variables are produced by the disk of gas (Gorbatzky 1964; Warner 1974; Nather and Robinson 1974), and we make the same suggestion for WZ Sge. If the disk is adequately represented by an "α-model" disk, then equation (5.9.6) in Novikov and Thorne (1973) gives an estimate for the optical depth perpendicular to the plane of the disk. Adopting $\alpha \approx 0.1$, and with $\dot{M} = 1 \times 10^{16}\ \mathrm{g\ s}^{-1}$, we find that the optical depth from the center to the surface of the disk due to free-free transitions should be $\tau_{\mathrm{ff}} \approx 400$. Thus the optical depth of the disk is very large, and we may expect the disk to mimic a stellar atmosphere. The spectrum of the disk will certainly be peculiar; but as a first approximation, let us assume that each small region of the disk has a spectrum similar to the spectrum of a normal stellar atmosphere with an effective gravity and temperature equal to the effective gravity and temperature of the photosphere at that region of the disk. The photosphere of the disk should be near $\tau_{\mathrm{ff}} = 1$. In the isothermal approximation the density, ρ, of the disk in the direction perpendicular to the disk, z, falls off as

$$\rho \propto \exp(-z^2/h^2) , \quad (14)$$

where h is the scale height of the disk. Since $d\tau_{\mathrm{ff}} = \kappa_{\mathrm{ff}}\rho dz \propto \rho^2 dz$, the optical depth integrates to unity at about 1.5 scale heights. The effective gravity at the photosphere is given by

$$g_e = \frac{GM_D Z}{r^3} \approx \frac{1.5GM_D h}{r^3} , \quad (15)$$

where r is the distance from the center of the disk. Referring once again to equation (5.9.6) of Novikov and Thorne (1973), we calculate $h/r \approx 0.013$, and the effective gravity of the photosphere lies in the range $4.0 < \log g_e < 6.0$. The effective temperature of the disk is calculated from equation (5.10.1) in Novikov and Thorne and lies in the range $6 \times 10^3 < T_e < 3 \times 10^4$, with the lower temperatures and gravities corresponding to the outer regions of the disk. In order to find the hydrogen line widths, we refer to the atmosphere calculated by Wickramasinghe (1972) for $\log g_e = 6$, $T_e = 25{,}000$ K, and for a solar abundance. In this model, the Hγ absorption line has wings which are easily traced to ± 70 Å from the line center. The lines will be further broadened by Doppler shifts owing to the Keplerian motion of the disk, which in WZ Sge can be up to $\pm 2300\ \mathrm{km\ s}^{-1}$, or ± 30 Å at Hγ. Thus the absorption wings should extend to ± 100 Å from the line center. The observed absorption wings in WZ Sge extend to ± 80 Å to ± 100 Å, and thus agree nicely with the widths we expect from the disk of gas. There is no need to require that the lines be produced by the white dwarf, and there is no need to require that the white dwarf be bright.

Let us now turn to the properties of the bright spot. The position of the spot was fixed, in part, by our *a priori* assumption of the validity of equation (5). However, the angle to the spot, α, is determined primarily by the observed value of the angle β, so our calculated value is very nearly independent of equation (5). Lubow and Shu (1975) calculate the position of the spot to be at $\alpha \approx 50°$ for $q = 20$. Our value of $\alpha = 56°$ is in fair agreement with theirs. The agreement is perhaps better if we consider that Lubow and Shu have calculated the position where the shock front is

first formed, but the true bright spot will extend downstream from the shock, to larger values of α. The extension of the spot downstream should be set by the product of the cooling time and the disk velocity. The disk velocity at the radius of the spot is 725 km s^{-1}. We identify the cooling time for material passing through the shock with the decay time for a flicker, or about 30 s. Thus the diameter of the spot in the plane of the disk should be about 2.2×10^9 cm, which agrees with the radius of 1.0×10^9 cm we have already determined from the eclipse solution. The midpoint of the spot is now displaced 6°.5 from the shock, which may account for the 6° discrepancy between the observed value of α, and the value predicted by Lubow and Shu.

There are two temperatures we may associate with the spot. One is the effective temperature, and is the temperature measured by the observer. The other is the central temperature, and is the temperature needed to discuss the vertical structure of the spot. The two temperatures are different if the spot is optically thick. The effective temperature, T_{se}, is calculated from

$$\sigma T_{se}^4 = L_{spot}/(\text{area}) = \frac{GM_D\dot{M}}{2d}\frac{1}{(\text{area})}, \quad (16)$$

where the area is the radiating surface of the spot. Since the spot is embedded in the disk, its radiating area is twice its cross section as seen from above the disk. We assume the cross section to be circular, with a radius equal to the extent of the spot in the plane of the disk as calculated from the cooling time scale: 1.1×10^9 cm. The radiating area is, then, 7.6×10^{18} cm^2, and the effective temperature of the spot is $T_{se} = 16{,}000$ K. We calculate the central temperature of the spot, T_{sc}, from the diffusion approximation:

$$\frac{d}{d\tau}(\tfrac{1}{3}acT_{sc}^4) = F = \frac{L_{spot}}{(\text{area})} = \sigma T_{se}^4, \quad (17)$$

where a is the radiation density constant, c is the speed of light, and F is the radiation flux density. To first order, equation (17) integrates to

$$T_{sc}^4 = \tau T_{se}^4. \quad (18)$$

It is not yet possible to calculate the optical depth of the spot, τ, from first principles. Instead, we suggest that the optical depth of the spot should be no less than the optical depth of the surrounding disk. We have already found the optical depth of the disk to be 400, and adopt here also $\tau = 400$. The resulting central temperature is $T_{sc} = 7.2 \times 10^4$ K.

In order to calculate the z dimension of the spot, we use the central temperature of the spot to calculate its scale height, and, following our previous arguments, we set the photosphere at 1.5 scale heights. If the spot is in hydrostatic equilibrium, its scale height, h_s, is approximately

$$h_s^2 = \frac{2P}{2}\frac{d^3}{GM_D} = \frac{2kT_{sc}}{\mu m_H}\frac{d^3}{GM_D}, \quad (19)$$

where P and ρ are the pressure and density of the spot, and k, μ, and m_H have their usual meanings. Equation (17) yields $h_s = 6.5 \times 10^8$ cm, and thus the height of the spot's photosphere, h_p, is $h_p = 9.8 \times 10^8$ cm. The height of the photosphere also agrees with the radius of 1.0×10^9 cm we determined from the eclipse solution. Perhaps more important, since the height of the spot and its extension in the plane of the disk are nearly equal, we appear to have been justified in assuming a circular cross section for the spot when we solved the primary eclipse.

The α-model predicts a scale height for the disk in WZ Sge of $h/r \approx 0.013$, or $h = 1.2 \times 10^8$ at the radius of the spot. Thus both the scale height and the photosphere of the spot are 5 times larger than we would normally expect for the disk at that radius. We suggest that the disk can retain this large scale height all of the way around its circumference. Immediately downstream from the spot, the disk cools and then begins to collapse exponentially to its normal height. The time scale for the collapse of the photosphere will be approximately

$$t \approx h_p c_s^{-1} = \left(\frac{h_p^2 \mu m_H}{\gamma kT}\right)^{1/2}, \quad (20)$$

where c_s is the sound speed and T the temperature of the disk after it has cooled downstream from the spot. The disk will cool rapidly ($\sim$30 s) until hydrogen begins to recombine, after which the disk will cool several orders of magnitude more slowly (Dalgarno and McCray 1972). Therefore we take $T = 10^4$ K, and the time scale for the collapse is $t \approx 550$ s. This collapse time will be a severe underestimate if there is significant turbulent pressure downstream from the spot, or if some of the gas transferred by the stream "splashes" to large z distances. The rotation period of the disk at the radius of the spot is about 850 s. Therefore the collapse time can be comparable with or larger than the rotation period, and the disk will not have a chance to collapse before it rotates back to the spot and is once again pushed to the large scale height. Lubow and Shu (1976) calculated the thickness of the stream in WZ Sge just prior to its impact with the disk and found it to be 3 to 4 times greater than the scale heights of a normal disk. They suggested that the stream would flow over the top and bottom of the disk. However, if the edge of the disk is, in fact, about 5 times thicker than expected for an α-model disk, as we have suggested, the thickness of the disk is greater than that of the stream, and the spillover will not occur.

The last major feature of the light curve is the dip which occurs near phase 0.3. Two pieces of evidence suggest that the dips are due to an obscuration of the spot. The first is that the dips give the visual impression that part of the W Ursae Majoris hump has been "chopped out." The second is that, according to Krzemiński and Smak (1971), the color change of WZ Sge during the dips is similar to the color change during primary eclipse. Our solution of the primary eclipse showed that the position of the spot varies

only slightly. Therefore the large changes in the phase at which the dips occur must be due to changes in the position of the obscuring body. Only clouds or blobs of gas appear to have this freedom of motion. We believe that these blobs are large-scale density fluctuations in the accretion disk. This location for the blobs provides a natural explanation for the time of occurrence and the time scale of the dips. Since the spot is near the outer edge of the disk, blobs in the disk can pass in front of and obscure the spot only when the spot is on the opposite side of the disk from the observer, which occurs between phases 0.2 and 0.4. Since the spot is fixed in the rotating reference frame of the binary system, but the material of the disk, including the blobs, is rotating rapidly, the blob can pass in front of the spot quite rapidly and can easily produce the extremely short "ingress" and "egress" times displayed by the dips. Variation in the size and shape of the blobs accounts for the variation in the size and shape of the dips. Such blobs may present theoretical problems, but a decision about whether such blobs are reasonable will have to wait until more sophisticated models for accretion disks are available.

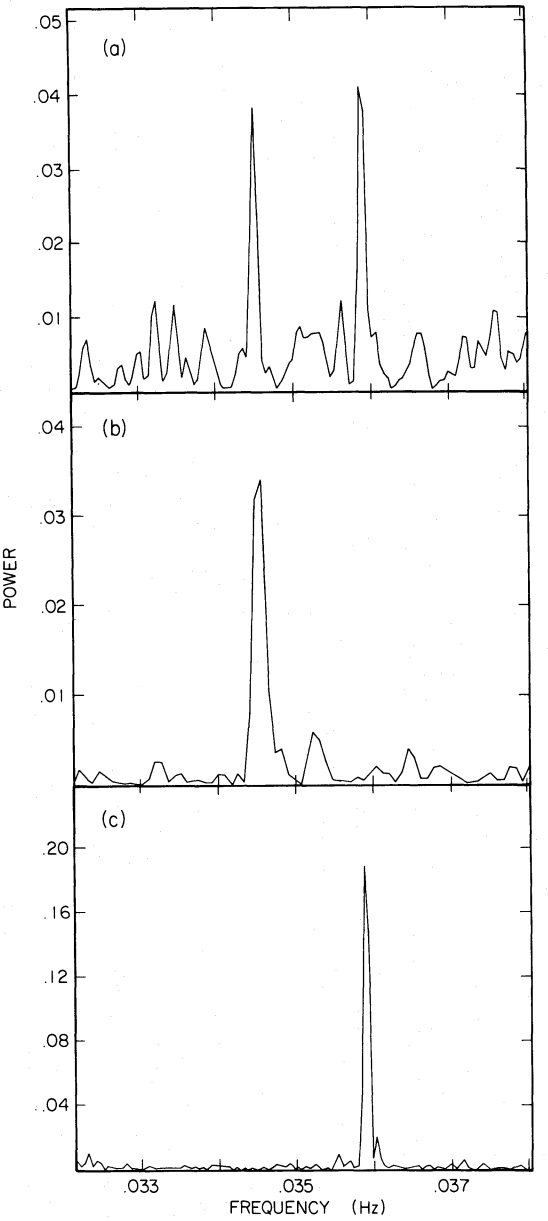

FIG. 7.—Power spectra of the light curves of WZ Sge: (*a*) run 1203, (*b*) run 1208, (*c*) run 1768. The two pulsations have periods $P_1 = 28.98$ s and $P_2 = 27.87$ s, and amplitudes of $A_1 = 0.0034$ mag and $A_2 = 0.0043$ mag.

V. THE WHITE-DWARF PULSATIONS

We have tested all of our light curves of WZ Sge for the presence of rapid coherent oscillations by taking their power spectra (Robinson and Warner 1972). The results were positive: every run except run 1203 had one coherent oscillation; run 1203 had two. Representative power spectra are shown in Figure 7, and the periods and amplitudes of the oscillations are listed in Table 4. The data in Table 4 show that the oscillations always have one of two periods; a period at $P_1 = 27.87 \pm 0.02$ s appears 7 times, and a period at $P_2 = 28.98 \pm 0.04$ s appears twice. The periods are very stable, having no detectable change on any time scale between 1 hour and 6 years. The 6 year scale time base for the 27.87 s oscillation yields an upper limit to the rate of change of the period of $|\dot{P}| < 3 \times 10^{-10}$ or $Q = |\dot{P}|^{-1} > 3 \times 10^9$. The amplitudes of the oscillations are clearly variable, but the nature of the amplitude variation is unusual. When the oscillations are visible their amplitudes are about $A_1 = 0.0043$ mag and $A_2 = 0.0034$ mag, and the run-to-run variations in the amplitudes are not significantly larger than the error in measurement. When the oscillations become invisible, their amplitudes must be very small; the best upper limit to an amplitude is 0.0001 mag for the 28.98 s pulsation during run 1768. Thus the amplitudes change by more than a factor of 30; but, in spite of over 24 hours of observations, we have never detected one of the changes taking place. The most we can say is that, based on runs 1203 and 1208, the transition from high to low amplitude takes place in less than 48 hours. The oscillations are very pure sine curves. During run 1768, none of the harmonics

TABLE 4

THE RAPID OSCILLATIONS IN WZ SAGITTAE

Run	JD 2440000+	Period (s)	Amplitude (mag)
1203.....	1208	27.85 ± 0.04	0.0037
		29.01 ± 0.04	0.0033
1208.....	1210	28.94 ± 0.04	0.0035
1736.....	2930	27.87 ± 0.02	0.0045
1739.....	2931	27.89 ± 0.02	0.0043
1760.....	3011	27.89 ± 0.02	0.0032
1768.....	3013	27.85 ± 0.02	0.0047
1770.....	3041	27.83 ± 0.04	0.0050
1773.....	3047	27.85 ± 0.03	0.0044

of the 27.87 s period had an amplitude greater than 0.075 of the amplitude of the fundamental.

The most interesting data are from run 1203. The power spectrum of run 1203, shown in Figure 7*a*, indicates only that each of the two oscillations must be present at one time or another during the run. We now show that both oscillations are simultaneously present throughout the entire run by finding the unmistakable signature of beating between the oscillations. Let us add together two sine curves with constant frequencies ω_1 and ω_2, and with constant amplitudes A_1 and A_2. The intensity variation of the sum is

$$I(t) = A_1 \sin \omega_1 t + A_2 \cos \omega_2 t , \quad (21)$$

which, after obvious manipulations, becomes

$$I(t) = A(t) \cos [0.5(\omega_1 + \omega_2)t - \phi(t)] , \quad (22)$$

with

$$A^2(t) = A_1^2 + A_2^2 + 2A_1A_2 \sin [(\omega_1 - \omega_2)t] , \quad (23)$$

and

$$\tan \phi(t) = \frac{A_1 + A_2 \tan [0.5(\omega_1 - \omega_2)t]}{A_2 + A_1 \tan [0.5(\omega_1 - \omega_2)t]} . \quad (24)$$

Thus the resultant intensity variation is a cosine curve with a frequency that is constant and equal to the average of the two individual frequencies. The amplitude and phase of the cosine curve undergo periodic variations given by equations (23) and (24). If the two sine curves have the same amplitude, which is nearly the case in WZ Sge, equation (23) becomes

$$A(t) = 2A_1 |\cos [0.5(\omega_1 - \omega_2)t]| , \quad (25)$$

and, since the amplitude is defined to be positive, the phase variation degenerates into a square wave with the same period as the amplitude variation, and a peak-to-peak variation of exactly 180°.

We measured the amplitude and phase variation of the sum oscillation in run 1203 by the simple expedient of fitting equation (22) to successive portions of the light curve by least squares. The period of the sine curve was $[0.5(P_1^{-1} + P_2^{-1})]^{-1} = 28.42$ s, and each successive portion of the light curve was 280 s long. The resulting values of $\phi(t)$ are plotted as filled circles in Figure 8. Also plotted in Figure 8 is the expected square wave variation of $\phi(t)$. It should be noted that the amplitude and wavelength of the square wave are predetermined at 180° and $[0.5(P_1^{-1} - P_2^{-1})]^{-1} = 1456$ s, respectively. The only free parameters available in fitting the square wave to the data are the zero-point offsets in time and phase. The amplitude variations are contaminated by noise in the light curve, so we have averaged the amplitude variation over all of the beat cycles. The average amplitude variations are plotted in Figure 9 along with a plot of equation (25). Both the observed and the expected variations are displaced vertically in the plot because of noise, which, if uncorrelated, always adds to the average amplitude. Figures 8 and 9 show that the fit of the expected phase and amplitude variations to the observed variations is very good. Clearly we are seeing beating, and therefore both oscillations must be present simultaneously. Furthermore, Figure 8 shows that the beating is present throughout the entire run, so both oscillations must also be present throughout the entire run.

The combination of short period and high Q eliminates all components of the WZ Sge system except the white dwarf as a source of the oscillations. The simultaneous existence of the two oscillations

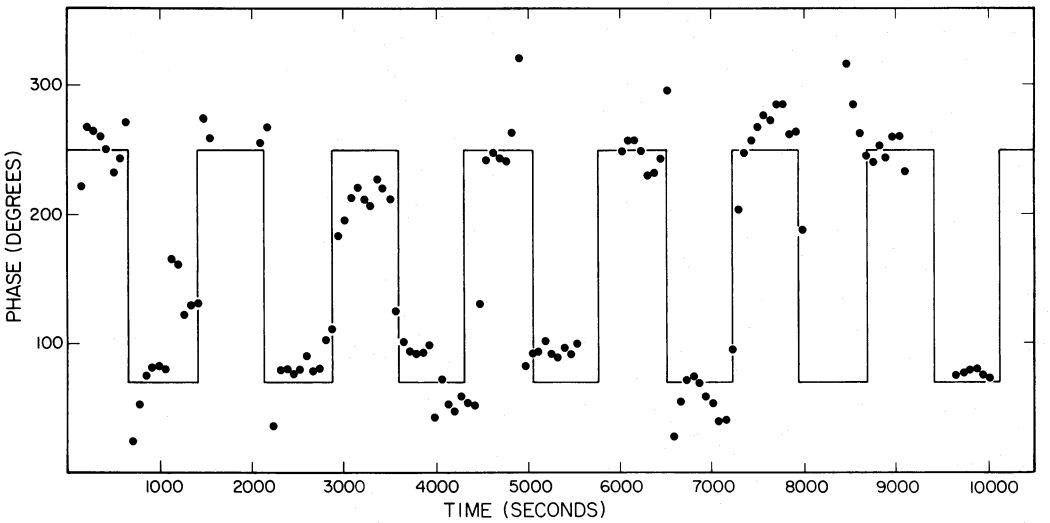

FIG. 8.—The O-C diagram for the pulsations during run 1203. The vertical axis is the difference in phase between the observed pulsations in run 1203 and a sinusoidal variation with a constant period of 28.425 s. *Dots*, observed residual. *Solid line*, residual that would be produced by beating if the 28.98 s and the 27.87 s pulsations are both present in the light curve of WZ Sge simultaneously.

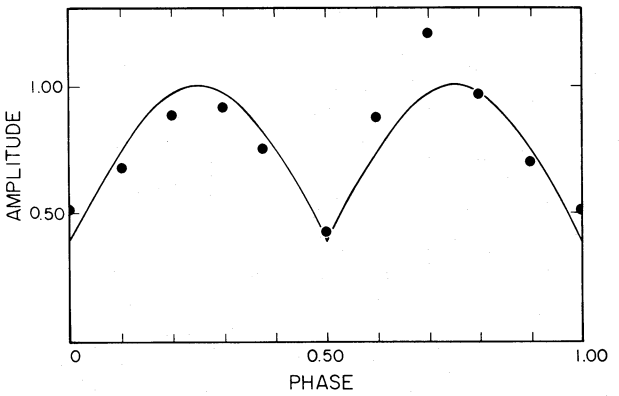

FIG. 9.—*Solid line*, predicted amplitude variation of a signal produced by beating two sine curves together in the presence of noise. *Dots*, average amplitude variation of the oscillation in the light curve of WZ Sge during run 1203. Figs. 8 and 9 together show that the 28.98 s and 27.87 s pulsations were simultaneously present throughout run 1203.

during run 1203 also eliminates rotation of the white dwarf as their sole source. Consider: If the oscillations were caused by spots on a rotating white dwarf, the simultaneous presence of two periods would require the white dwarf to be rotating differentially. If the white dwarf were rotating differentially, the spots would soon be destroyed by shearing, and it would no longer be possible to account for the high Q of the oscillations. Therefore we conclude that the oscillations in WZ Sge must be caused by pulsations of the white dwarf. The assignment of the oscillations to pulsations of the white dwarf is in agreement with our earlier conclusions that the white dwarf is a minor contributor to the total luminosity of WZ Sge. Even if the white dwarf contributes as little as 2% of the luminosity, its light need only be modulated by 15% to 20% to give the observed amplitude of the pulsations. The pulsating white dwarfs which are not in close binary systems have no difficulty in achieving magnitude variations this large (McGraw and Robinson 1975, 1976; Robinson 1976*b*).

The pulsations in WZ Sge have too long a period to be radial pulsations. We have already measured the mass of the white dwarf to be 0.38 $M_\odot$, and in order for the white dwarf to contribute less than 10% of the luminosity of WZ Sge, its effective temperature must be less than about 12,000 K. The period of the fundamental radial pulsation of a white dwarf with this mass and temperature is less than 20 s (Hubbard and Wagner 1970). The periods of radial pulsations in white dwarfs are sensitive to the mass of the white dwarf, but relatively insensitive to its temperature and chemical composition. Thus, if we wish to identify the 29 s pulsation as the fundamental radial pulsation, the mass of the white dwarf would have to be reduced to about 0.25 $M_\odot$, which is unacceptably different from the measured mass. In fact, neither the 28.98 s nor the 27.87 s pulsation can be the fundamental radial pulsation. The period spacing of radial pulsations is approximately $\Delta P/P \approx \Delta k/k$, where k is the overtone index. Using this relation, we find that the close spacing of the two periods would require that the pulsations be about the 25th-overtone pulsation. The fundamental radial pulsation period would then be several hundreds of seconds, and the mass of the white dwarf could be no more than a few hundredths of a solar mass —an even more severe disagreement with the measured mass. Therefore the pulsations must be nonradial pulsations. The theory of nonradial pulsations is not in a state that allows an unimpeachable identification of the pulsation mode, but it is clear that nonradial pulsations can easily account for the close spacing of the pulsation periods, and it is equally clear that at least one branch of the nonradial pulsations, the *g*-modes, has pulsation periods which can be longer than the radial pulsation periods. We conclude that the rapid oscillations in WZ Sge must be white-dwarf pulsations, that the pulsations cannot be radial pulsations, and that the pulsations could possibly be nonradial *g*-mode pulsations.

VI. SUMMARY AND DISCUSSION

The model we have presented for WZ Sge is qualitatively similar to the model developed by Krzemiński and Smak (1971); the geometry of the model is shown in Figure 5. There are significant quantitative differences between our model and that of Krzemiński and Smak which are due primarily to our recognition that the eclipse of the bright spot by the late-type star is a total eclipse, not a partial eclipse. We calculate the mass of the white dwarf to be 0.38 $M_\odot$, the mass of the late-type star to be 0.019 $M_\odot$, their separation to be 3.2×10^{10} cm, and the mass-transfer rate to be 1×10^{16} g s^{-1}. The remaining parameters of the model are listed in Table 3. An important feature of our model is that the white dwarf is only a minor contributor to the total optical luminosity of WZ Sge. What appear to be white-dwarf absorption lines in the spectrum of WZ Sge are, in fact, produced by the optically thick accretion disk around the white dwarf. In addition, we have detected rapid coherent oscillations in the light curve of WZ Sge with periods of 28.98 s and 27.87 s, thus making WZ Sge the first recurrent nova in which such oscillations have been found. On one occasion both periods were present simultaneously in the light curve. We used this fact to show that the oscillations must be white-dwarf pulsations, and cannot be caused by rotation of a spotted white dwarf. Using the observed mass of the white dwarf and the close spacing of the periods, we eliminated radial pulsations, and suggested that the pulsations could be nonradial *g*-mode pulsations.

As our final point, we shall examine the evolutionary state of WZ Sge. The late-type star cannot be a helium white dwarf, nor can it have a degenerate helium core. Its present envelope is hydrogen-rich, since the spectrum of the accretion disk, which is envelope material, contains only hydrogen and no helium lines. Therefore, any degenerate helium core which the late-type star now has, or ever had, must have a mass less than the total present mass of the star, or $M_{\rm core} \lesssim 0.019\ M_\odot$. The Chandrasekhar-Schönberg limit then

places an upper limit on the mass of the progenitor of the degenerate core of about 0.2 to 0.3 $M_\odot$. Stars with masses this low cannot have evolved in the lifetime of the universe, so the degenerate helium core can never have been formed. We do not exclude, of course, the possibility of significant depletion of hydrogen in the core by nuclear burning. Even so, the past evolution of the late-type star is limited to only two possibilities: either the late-type star has always had a low mass; or, if it ever had a high mass, it lost the mass too rapidly to permit total exhaustion of its core hydrogen. Since the mass of the late-type star is too low to permit hydrogen burning in the core, and since the lack of a degenerate helium core prevents hydrogen burning in a shell, the late-type star has no source of nuclear energy. There are only two possibilities for the structure of the late-type star: either it is not in thermal equilibrium, or it is a hydrogen-helium white dwarf. The latter possibility appears to be more nearly correct. The mass and radius of the late-type star fit the mass-radius relation for degenerate hydrogen-helium stars in which hydrogen content, X, has been reduced to about 0.1 (Faulkner 1971).

What drives the mass transfer in WZ Sge? There is no nuclear evolution forcing the radius of the late-type star to increase, and the mass ratio of the system is too large to allow thermal instabilities, of the sort which occur in Algol systems, to drive mass transfer. Paczyński (1967) and Faulkner (1971) have suggested that gravitational radiation removes orbital angular momentum from the system, decreases the separation of the stars, and thus forces mass transfer. We can compare our results directly with Paczyński's prediction, since Paczyński assumed that the late-type star was degenerate. Table 3 of Paczyński (1967) predicts a mass-transfer rate of about 6×10^{14} g s^{-1} for $X = 0.1$. Thus, gravitational radiation fails to account for the observed transfer rate of 1×10^{16} g s^{-1} by almost two orders of magnitude. The following argument shows that this result does not depend strongly on the adopted structure of the late-type star. We may calculate a time scale, t_{GR}, for the removal of orbital angular momentum, J, by gravitational rotation by setting $t_{GR} = J/\dot{J}$, where $\dot{J}$ is the rate of orbital angular momentum loss due to gravitational radiation. The orbital angular momentum of WZ Sge is about 4.7×10^{49} g cm^2 s^{-1}, and equation (5) given by Paczyński (1967) yields $\dot{J} = 8.3 \times 10^{31}$ g cm^2 s^{-2}. Thus, the time scale for evolution due to gravitational radiation is $t_{GR} = 1.8 \times 10^{10}$ yr. On the other hand, the observed evolutionary time scale of the mass transfer is $M_R/\dot{M} = 1.2 \times 10^8$ yr. Again, it would seem that gravitational radiation fails by more than two orders of magnitude to account for the observed rate of evolution of WZ Sge.

By default, we suggest that the mass transfer in WZ Sge must be driven by mass loss from the system. The mass loss must be more or less continuous, and the angular momentum per unit mass carried away must be greater than the mean angular momentum per unit mass of the system. We envision that the mass loss is a natural consequence of the mass-transfer process: mass loss drives the mass transfer which in turn drives the mass loss. The mass-loss rate need not be large, and even if it were comparable to the mass-transfer rate, $\sim 10^{-10}\ M_\odot$ yr^{-1}, the lost mass would not be detectable by now available observational techniques.

Further evolution of WZ Sge should hold no surprises. If mass loss continues to drive mass transfer, WZ Sge will last for a few 10^8 yr; if gravitational radiation eventually comes to dominate the mass transfer, WZ Sge will last somewhat longer. In either case, the end result must be that the late-type star lose all of its mass, leaving a single white dwarf. The white dwarf will be quite ordinary: beyond causing a few superficial nova eruptions, the mass of the late-type star is insufficient to disequilibriate the white dwarf in any significant way.

We thank David Meier for many illuminating discussions on the subject of accretion disks. It is a pleasure to acknowledge an extended correspondence with J. E. Pringle, who is developing an independent and alternative model for WZ Sge. This research was supported in part by NSF grants AST 75-15124 and AST 76-23882.

REFERENCES

Dalgarno, A., and McCray, R. A. 1972, *Ann. Rev. Astr. Ap.*, **10**, 375.
Faulkner, J. 1971, *Ap. J. (Letters)*, **170**, L99.
Flannery, B. 1975, *M.N.R.A.S.*, **170**, 325.
Greenstein, J. L. 1957, *Ap. J.*, **126**, 23.
Gorbatzky, V. G. 1964, *Astr. Zh.*, **41**, 849.
Huang, Su-Shu. 1972, *Ap. J.*, **171**, 549.
Hubbard, W. B., and Wagner, R. L. 1970, *Ap. J.*, **159**, 93.
Humason, M. L. 1938, *Ap. J.*, **88**, 228.
Kraft, R. P. 1961, *Science*, **134**, 1433.
———. 1964, *Ap. J.*, **139**, 457.
Kraft, R. P., Mathews, J., and Greenstein, J. L. 1962, *Ap. J.*, **136**, 312.
Krzemiński, W., and Kraft, R. P. 1964, *Ap. J.*, **140**, 921.
Krzemiński, W., and Smak, J. 1969, in *Non-Periodic Phenomena in Variable Stars*, ed. L. Detre (Budapest: Academic Press), p. 371.
———. 1971, *Acta Astr.*, **21**, 133.
Lubow, S. H., and Shu, F. H. 1975, *Ap. J.*, **198**, 383.
———. 1976, *Ap. J. (Letters)*, **207**, L53.
Mayall, M. W. 1946, "Bull. Harvard Col. Obs.," No. 918, p. 3.
McGraw, J. T., and Robinson, E. L. 1975, *Ap. J. (Letters)*, **200**, L89.
———. 1976, *Ap. J. (Letters)*, **205**, L155.
McLaughlin, D. B. 1953, *Ap. J.*, **117**, 279.
Mumford, G. S. 1969, in *Mass Loss from Stars*, ed. M. Hack (New York: Springer-Verlag), p. 204.
———. 1971, *Ap. J.*, **165**, 369.
———. 1974, *Inf. Bull. Variable Stars*, No. 889.
Nather, R. E. 1973, *Vistas in Astronomy*, Vol. **15**, p. 91.
Nather, R. E., and Robinson, E. L. 1974, *Ap. J.*, **190**, 637.
Nather, R. E., and Warner, B. 1971, *M.N.R.A.S.*, **152**, 209.
Novikov, I. D., and Thorne, K. S. 1973, in *Black Holes*, ed. C. de Witt (New York: Gordon & Breach), p. 344.
Paczyński, B. 1967, *Acta Astr.*, **17**, 287.
Plavec, M., and Kratochvil, P. 1964, *Bull. Astr. Inst. Czechoslovakia*, **15**, 165.
Robinson, E. L. 1976*a*, *Ann. Rev. Astr. Ap.*, **14**, 119.
———. 1976*b*, *Proc. Los Alamos Conf. Solar and Stellar Pulsations*, p. 98.

Robinson, E. L., and Warner, B. 1972, *M.N.R.A.S.*, **157**, 85.
Smak, J. 1969, *Acta Astr.*, **19**, 155.
———. 1976, *Acta Astr.*, **26**, 277.
Warner, B. 1973, *M.N.R.A.S.*, **162**, 189.
Warner, B. 1974, *M.N.R.A.S.*, **168**, 235.
Warner, B., and Nather, R. E. 1972, *M.N.R.A.S.*, **156**, 297.
Wickramasinghe, D. T. 1972, *Mem. R.A.S.*, **76**, 129.

R. EDWARD NATHER, JOSEPH PATTERSON, and EDWARD L. ROBINSON: Department of Astronomy, The University of Texas, Austin, TX 78712